JOC The Journal of Organic Chemistry

Article

pubs.acs.org/joc

Synthesis, Structure and Metal Binding Property of Internally 1,3-Arylene-Bridged Azacalix[6]aromatics

Yi-Xin Fang,[†] Liang Zhao,*[,‡] De-Xian Wang,[†] and Mei-Xiang Wang*[,‡]

[†]Beijing National Laboratory for Molecular Sciences, CAS Key Laboratory of Molecular Recognition and Function, Institute of Chemistry, Chinese Academy of Sciences, Beijing 100190, China

[‡]Key Laboratory of Bioorganic Phosphorus Chemistry & Chemical Biology (Ministry of Education), Department of Chemistry, Tsinghua University, Beijing 100084, China

Supporting Information

ABSTRACT: Three internally 1,3-arylene-bridged azacalix[6]aromatics **1**−**3** were synthesized by the Pd-catalyzed macrocyclic fragment coupling reaction between a stellated dibrominated pentamer and N^2,N^6-dimethylpyridine-2,6-diamine or N^1,N^3-dimethylbenzene-1,3-diamine. Single-crystal X-ray analysis revealed that these bimacrocyclic compounds all adopt a triply pillared groove-shaped conformation, conceptually being derived from the fusion of two 1,3-alternate macrocycles. Four host/metal discrete complexes of the all-pyridine host **1**, $\{Co(\mathbf{1})(CH_3OH)_2\}(CoCl_4)\cdot 3(CH_3OH)$, $\{Ni(\mathbf{1})(CH_3OH)_2\}(NiCl_4)$, $\{Ni(\mathbf{1})(CH_3OH)_2\}(ClO_4)_2\cdot CH_3OH$ and $\{Cd_2(\mathbf{1})(CH_3CN)_4(H_2O)_4\}(ClO_4)_4$, have been structurally characterized by X-ray crystallographic analysis, exploring two different metal binding modes. The metal complexation property of the host **1** in solution was then investigated by the UV-vis and NMR titration. With variation of the radii of the tested metal ions (Mn^{2+}, Fe^{2+}, Co^{2+}, Ni^{2+}, Cu^{2+}, Zn^{2+}, Cd^{2+}, and Hg^{2+}), the host **1** can trap one or two metal ions via four different modes by using its two coordination cavities or two marginal pyridine rings. Such metal binding diversity of internally bridged heteracalixaromatics spotlights their potential applications in metal ion transport, ion channel, and metallo-enzyme mimics.

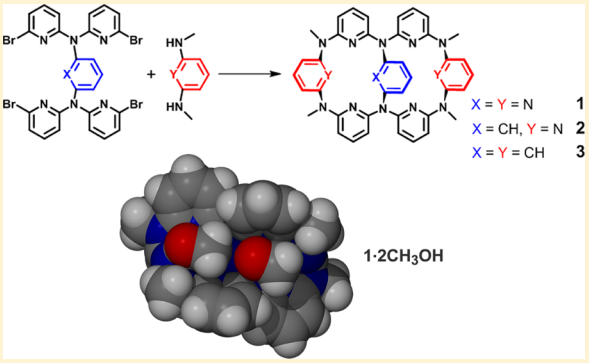

INTRODUCTION

The synthesis and property studies of new macrocyclic compounds have been a research focus in host−guest chemistry because of their extensive applications from ion transport,[1] chemosensing and imaging,[2] and catalysis[3] to nuclear waste treatment.[4] Heteracalixaromatics, a new generation of macrocyclic host molecules with heteroatoms in place of the bridging methylene moieties in conventional calixarenes, have received growing attention in recent years.[5] Because of different electronic nature of heteroatoms (such as O[6] and N[5e,7]) from the sp^3 carbon in conventional calixarenes, these heteroatom-bridged calix(hetero)aromatics exhibit exceptional structural tunability and interesting molecule and ion recognition properties.[5,8] Among them, azacalix[*n*]pyridines have exhibited comprehensive molecular recognition properties due to the coordination and hydrogen-bonding receptor nature of their multinitrogen-containing skeletons.[5c] For example, tetramethylazacalix[4]pyridine has been utilized in recognizing various metal cations[9] and neutral molecules (both aromatic and aliphatic diols and monools)[10] by its dominant 1,3-alternate conformation and its protonated form can accommodate diverse anionic guests of different size and geometry as well.[11] However, although the larger homologues of azacalix[4]pyridine have been successfully synthesized by us in comparable yields,[7d] their practical applications in molecular recognition become increasingly difficult along with the size expansion of macrocycles due to their highly flexible and fluxional conformations.

Recently, Osuka and co-workers introduced an internally bridged 1,4-phenylene group into an expanded porphyrin system in order to suppress the intrinsic twisting of such macrocycles with increasing number of pyrrolic subunits.[12] We thus envisioned that this bridging method may be applicable in stabilizing the conformation of the large azacalixaromatics and thus facilitates their potential applications in molecular recognition. This bimacrocyclic arrangement can be described as the fusion of two regular azacalixaromatics, possibly exhibiting specific metal ion recognition properties and providing a bimetallic cavity for metalloenzyme mimic[13] and the development of new bifunctional catalysts.[14] We report herein the synthesis of three internally 1,3-arylene-bridged azacalix[6]aromatics **1**-**3**, in which the 1,3-arylene bridging unit was found to bisect and resultingly fix the macrocycles of azacalix[6]aromatics based on single crystal X-ray analysis and NMR studies. The all-pyridine host **1** was screened for its ability to bind a series of metal ions using UV−vis titration, wherein the 1:1 and 1:2 host-metal binding stoichiometries were observed. Further NMR investigation and crystal structure

Received: July 30, 2012
Published: October 28, 2012

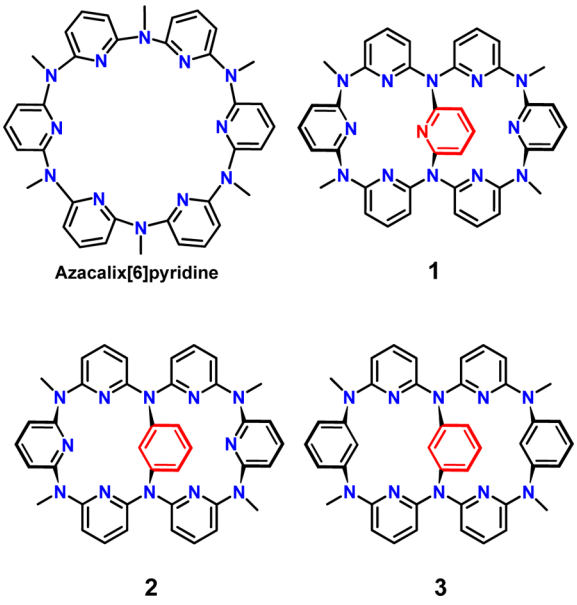

studies of four **1**·metal complexes explored four different metal binding modes of **1**.

RESULTS AND DISCUSSION

Synthesis of Internally 1,3-Arylene-Bridged Azacalix[6]-aromatics 1−3. Retrosynthetically, the disconnection of the target molecule **1**, an azacalix[6]pyridine internally bridged by a pyridine ring, mainly leads to two promising routes (Scheme 1). The first possible route (approach I) refers to the coupling between a $(NH)_2(NMe)_2$-bridged calix[4]pyridine compound **4** and a α,ω-dibromonated linear trimer **5**. However, the Pd-catalyzed Buchwald−Hartwig coupling reaction[15] between **4** and **5** at 110 °C in toluene in the presence of bis(diphenylphosphino)propane (dppp) as a ligand and NaO^{t}Bu as a base only produced the desired compound **1** in a quite low yield of 5%. MALDI-TOF mass spectra revealed that main isolated products formed in this reaction are the oligomers of **4** and **5**. This implies that the macrocyclization step is unfavored, which can be rationalized by the fact that it is difficult to simultaneously introduce two triarylamine moieties into a macrocycle due to the steric hindrance.

We then divided compound **1** into three fragments (approach II), two 2,6-diaminated pyridine units of **6** and a stellated N-bridged pyridine pentamer **7**, with a consideration that the early introduction of the bulky triarylamine moieties into the coupling fragments may improve the final-step macrocyclization yield of **1**. The preparation of the NH-bridged α,ω-dibrominated linear trimer **11** was made possible in 81% yield by the nucleophilic substitution reaction between 2,6-diaminopyridine **8** and 2,6-dibromopyridine **10** with KO^{t}Bu as a base. However, this kind of nucleophilic substitution reaction is not applicable for the synthesis of the key building block **7** even using sodium hydride as a strong base. We then adopted the CuI-mediated Ullmann coupling reaction of **10** and **11** to prepare **7** (Scheme 2). After optimizing reaction conditions, a yield of 33% for compound **7** was finally achieved by operating the reaction at 100 °C in dimethylformamide (DMF) in the presence of NaH as a base. When the NH-bridged arene trimer analogue **12** was employed for the synthesis of the pentamer **13**, the loading amount of CuI can be lowed to 10% mol and a moderate yield of 51% was acquired by performing the reaction in dimethyl sulfoxide (DMSO) in the presence of K_2CO_3 and phenanthroline as a base and an additive, respectively.

With the stellated tetrabromide compounds **7** and **13** in hand, we carried out their macrocyclization reaction with the diaminated compounds **6** and **14** by different combinations in order to produce three internally bridged calixaromatic targets **1**-**3**. In our previous work on the synthesis of azacalix[n]pyridines, the Pd-catalyzed Buchwald−Hartwig coupling reaction has shown high efficiency in the final macrocyclization step.[7d] Under similar conditions using $Pd_2(dba)_3$ (10 mol %), dppp (20 mol %), and NaO^{t}Bu (3 equiv), substrates **6** and **7** were refluxed in toluene for 6 h to afford the desired product **1** in a yield of 34% (Table 1, entry 1). Further elevating the amount of **6** can not improve the yield of **1**, which instead resulted in more oligomeric products. In contrast, the yields of the macrocyclization reactions between the arene-contained stellated pentamer **13** and the diaminated compound **6** or **14** can be enhanced upon increasing the amount of the diaminated reactant (Table 1, entries 4 and 7). In these two reactions, high dilution is not required to prevent polymerization (Table 1, entry 5). This is probably ascribed to the conformation difference of **7** and **13** derived from different conjugation scenarios between the central pyridine ring (for **7**) or arene ring (for **13**) and its adjacent bridging nitrogen atoms. We hypothesize that the yield difference between **1** and **2**−**3** may originate from the influence of the electron-rich phenylene ring in **13**, which is more favored

Scheme 1. Retrosynthetic Analysis of the 1,3-Pyridyl-Bridged Azacalix[6]pyridine 1

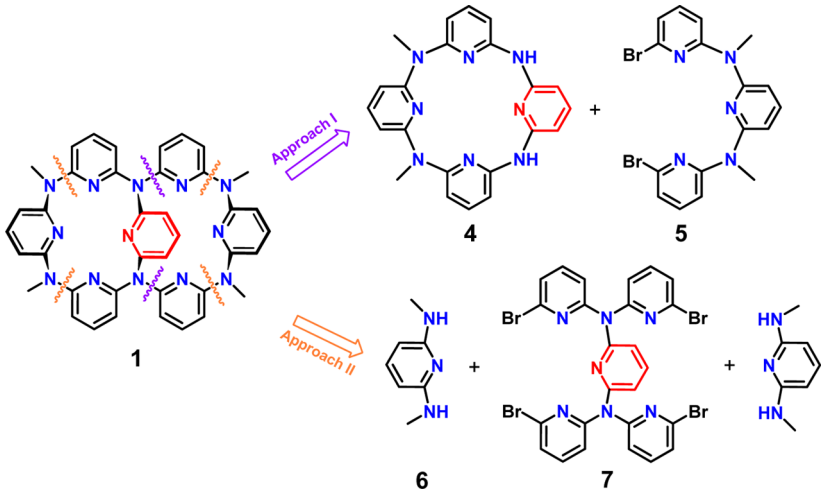

dx.doi.org/10.1021/jo301528f | J. Org. Chem. 2012, 77, 10073−10082

Scheme 2. Synthesis of the Stellated Pentamers 7 and 13

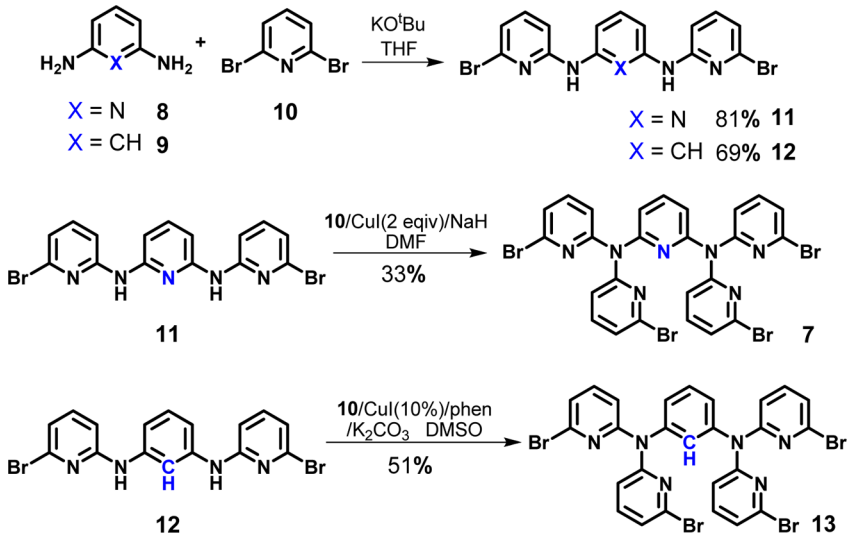

Table 1. Synthesis of the Internally 1,3-Arylene-Bridged Azacalix[6]aromatics 1−3

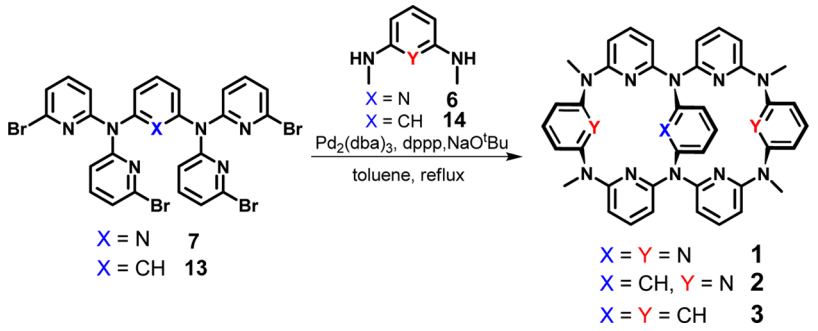

entry	reactant		ratio[a]	product	yield[b] (%)
1	7	6	0.55:1	1	34
2	7	6	1:6	1	26
3	13	6	0.55:1	2	36
4	13	6	1:6	2	51
5	13	6	1:6[c]	2	49
6	13	14	0.55:1	3	29
7	13	14	1:6	3	48

[a]Reaction conditions: 10 mol % of $Pd_2(dba)_3$, 20 mol % of dppp, 3 equiv NaO^{t}Bu, refluxing in toluene. [b]Isolated yield. [c]Concentrations of **13** and **6** are 1.1×10^{-2} M and 6.6×10^{-2} M, respectively.

for the Buchwald−Hartwig reaction than the electron-deficient pyridine-containing compound **7**.

Structural Characterization of 1−3. The molecular structures of **1−3** were first established by X-ray crystallography. Single-crystal X-ray crystallographic studies revealed that compounds **1−3** each featuring a bicyclic scaffold adopt a juxtaposed 1,3-alternate conformation. As shown in Figure 1, four procumbent pyridine rings in each compound constitute a groove through the bridging of three central vertical aromatics, which are parallel to each other but no $\pi-\pi$ stacking therein. Each N-Me bridging nitrogen atom in **1−3** exhibits a sp^2 electron configuration with the summation of three ∠C−N−C bond angles close to 360°. A pair of nitrogen atoms of the triarylamine $N(Ar)_3$ moieties in **1−3** (such as N6 and N8 in **1**) were found to display significant sp^2 feature with a ∠C−N−C bond angle summation of 360° but involving almost isometric C−N bong lengths. Because of severe steric hindrance between aromatic rings in such triarylamine moieties, an outward $\angle C_{pyridine}-N-C_{pyridine}$ angle of each triarylamine nitrogen atom (highlighted in red in Figure 1) is approximately 124°, larger than the rest ∠C−N−C angles for the bridging nitrogen atoms in the range of 117−120°. In addition, conjugation scenarios between these bridging nitrogen atoms and adjacent aromatic rings are also different in **1−3**. The bridging nitrogen atoms conjugate well with the procumbent pyridine rings in each compound case, while as to the vertical aromatics the conjugation between the bridging nitrogen atoms and the electron deficient pyridine rings is better than that of the phenyl rings. It is noteworthy that two methanol molecules are accommodated within the groove of compound **1** through the hydrogen bonds at O1···N3 = 2.917 (4) Å and O2···N7 = 2.902 (4) Å. In contrast, compound **2** only weakly interacts with a dichloromethane molecule (the occupancy ratio is 0.25) by a C−H···N hydrogen bond. Compound **3** exhibits no solvent molecule recognition based on its crystal structure. This observation spotlights the advantage of the all-pyridine compound **1** in molecular recognition due to its multiple bonding sites of coordination and hydrogen bonding.

dx.doi.org/10.1021/jo301528f | J. Org. Chem. 2012, 77, 10073−10082

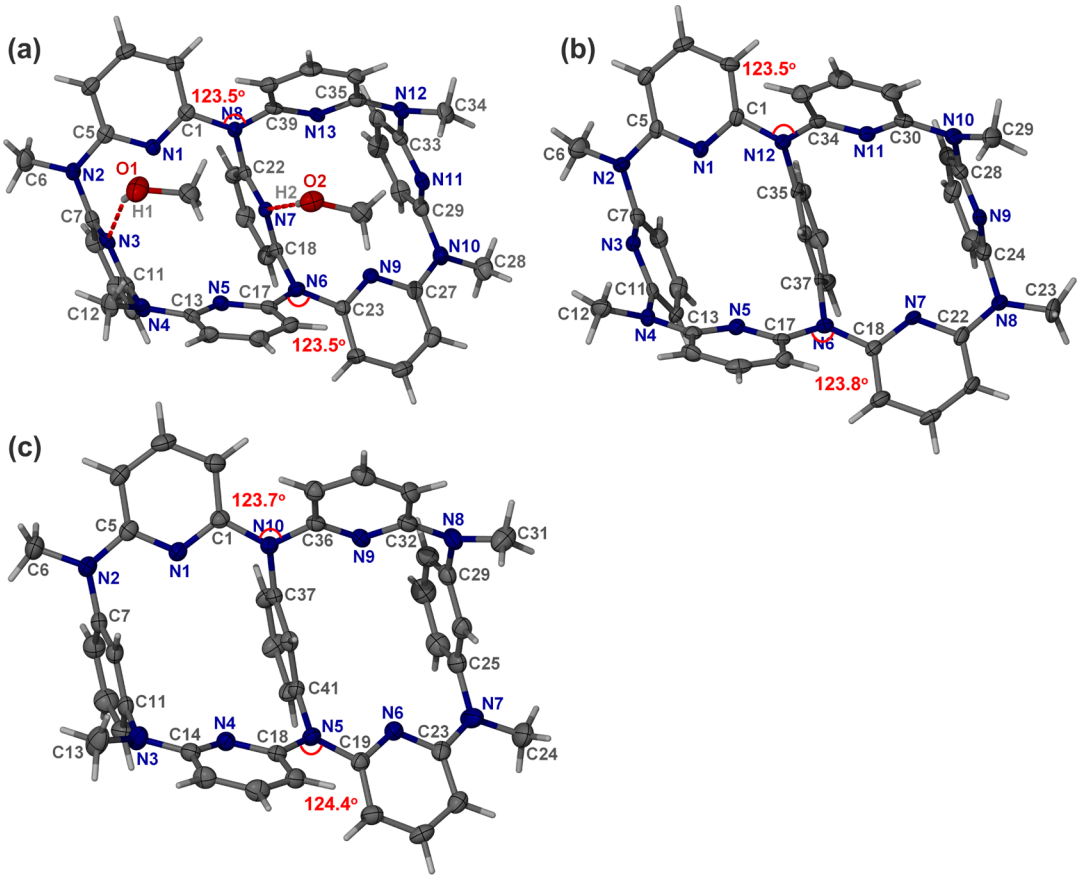

Figure 1. Crystal structures (thermal ellipsoids at the 50% probability level) of (a) **1**·2CH_3OH, (b) **2**·0.25CH_2Cl_2 (dichloromethane molecule is omitted for clarity), and (c) **3**. Color scheme for atoms: C black, H gray, O red, N blue.

Structural investigation of **1**−**3** in solution was carried out with one- and two-dimensional NMR spectroscopy (Figures S5−S19, Supporting Information). The ^1H and ^{13}C NMR signals of **1**−**3** are consistent with a C_2-symmetrical conformation shown in their crystal structures. Upon the gradual introduction of the electron-rich 1,3-phenylene ring into the bicyclo skeleton from **1** to **3**, the characteristic singlet peak of the bridging N-Me moiety undergoes a slight upfield shift from 3.31 ppm for **1**, through 3.28 ppm for **2** to 3.25 ppm for **3**. Although the three central vertical aromatic rings in **1**−**3** have poor conjugation with their adjacent bridging nitrogen atoms in comparison with the four procumbent rings reflected by their crystal structures, the resonance peaks of the protons on such three central rings are instead at an upfield region. This is possibly associated with a parallel face-to-face arrangement of the vertical rings. In that way, every vertical ring is situated on the shielding region of the other two. This rationale is also applicable to an approximately 0.4 ppm chemical shift difference between H_c and H_e as shown in Figure 2. It is obvious that each H_e of one pyridine ring (**I**) is located at the deshielding position of the adjacent procumbent pyridine ring (**I**′). From the variable-temperature proton NMR of **1** (Figure 2), we found that the resonance of H_f and H_g both experience an upfield shift (0.14 and 0.06 ppm, respectively) upon decreasing the temperatures from 298 to 198 K whereas the rest proton peaks only have a small shift. A similar NMR peak variation is observed as well in the variable-temperature proton NMR spectra of **2** and **3** (Figures S20 and S21, Supporting Information). This observation imply that the conformation of the internally bridged calix[6]aromatics **1**−**3** are so rigid that only the central aromatic ring can adjust its position very slightly.

Crystal Structures of Four 1·Metal Complexes. Since compound **1** is constituted all by pyridine rings, we expect it is suitable for metal ion recognition by metal-pyridine coordination. The phenylene-bridged compounds **2** and **3** may diminish such coordination effects due to the steric hindrance of the C−H fragment on the phenyl rings. In this regard, the coordination chemistry of dipyridylamine analogues have been extensively investigated in the past several decades, which can be employed as molecular strings,[16] luminescent materials,[17] or afford a platform for organometallic chemistry studies.[18] As a polydentate bimacrocycle, compound **1** is likely capable of being a host to entrap one or two metal ions. Our attempt to crystallize some host/metal complexes of **1** in order to facilitate our comprehension of the binding modes between **1** and different metal ions led to four **1**·metal complexes.

When the host **1** was individually mixed in 1:4 ratio with metal salts ($CoCl_2$, $NiCl_2$, $Ni(ClO_4)_2$ and $Cd(ClO_4)_2$) to achieve saturated coordination, four **1**·metal complexes were acquired and their X-ray quality crystals were then deposited by a solvent diffusion or evaporation method. As shown in Figure 3a, the **1**·$CoCl_2$ complex is a binuclear complex with the formula of $\{Co(\mathbf{1})(CH_3OH)_2\}$-$(CoCl_4)\cdot 3(CH_3OH)$, in which the cationic part contains a cobalt center situated inside a cavity of **1** and the counteranionic species is a tetrahedral $[CoCl_4]^{2-}$ ion. The cobalt center Co1 is coordinated to four pyridyl nitrogen atoms of **1** (N1, N3, N5 and N7) [Co−N = 2.074(3)−2.114(3) Å] and two methanol molecules [Co−O = 2.088(3)−2.128(3) Å]. The Co−N distances are comparable to the

dx.doi.org/10.1021/jo301528f | J. Org. Chem. 2012, 77, 10073−10082

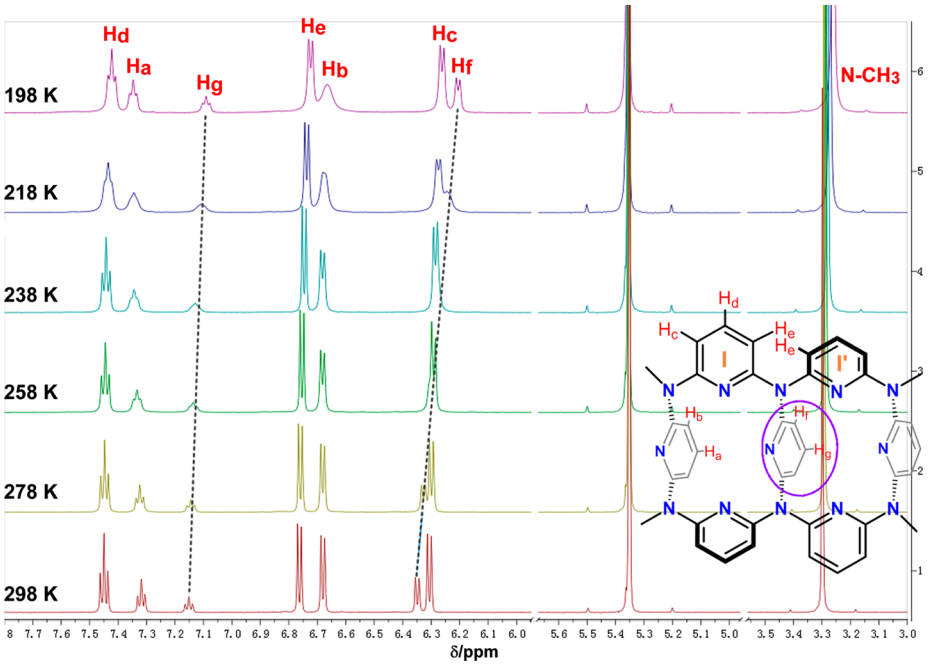

Figure 2. ^{1}H NMR spectra (600 MHz, CD_2Cl_2) of compound **1** at different temperatures.

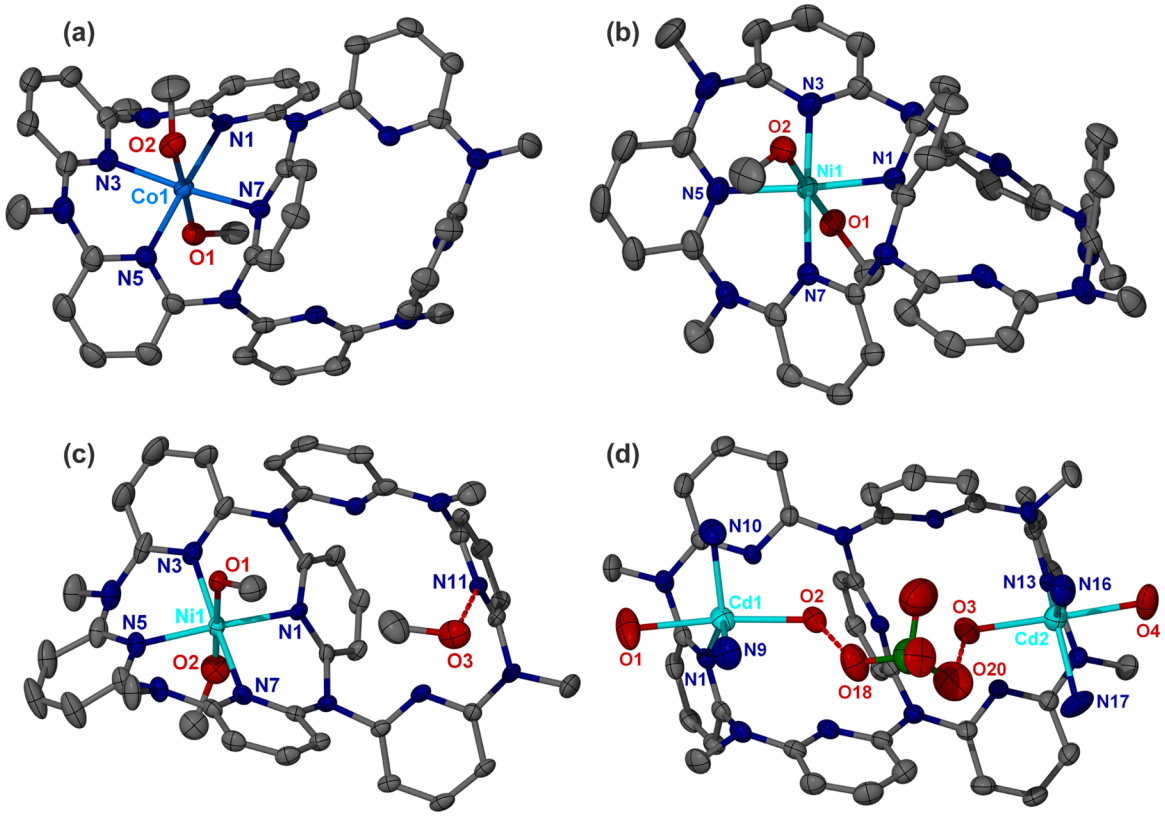

Figure 3. Crystal structures of four **1**·metal complexes (50% thermal ellipsoid probability level): (a) $\{Co(\mathbf{1})(CH_3OH)_2\}(CoCl_4)\cdot 3(CH_3OH)$. The anionic $[CoCl_4]^{2-}$ species and three peripheral methanol molecules are omitted for clarity. (b) $\{Ni(\mathbf{1})(CH_3OH)_2\}(NiCl_4)$. The anionic $[NiCl_4]^{2-}$ species is omitted for clarity. (c) $\{Ni(\mathbf{1})(CH_3OH)_2\}(ClO_4)_2\cdot CH_3OH$. Two perchlorate anions are omitted for clarity. The acetone molecule (O10) and a pyridine ring (N5) of **1** are disordered at two positions. Only one set of positions is shown here. (d) $\{Cd_2(\mathbf{1})(CH_3CN)_4(H_2O)_4\}(ClO_4)_4$). Three other perchlorates are omitted for clarity. The perchlorate shown in this figure is disordered at two positions. Only one set of positions is shown here.

bond lengths of a previously reported cobalt complex of *N*,*N*′-bis(α-pyridyl)-2,6-diaminopyridine (tripyridyldiamine, tpda).[19] The coordination environment of the cobalt ion in this **1**·$CoCl_2$ complex can be described as an octahedral 6-coordinated mode. The host molecule **1** underwent a significant conformation modification from its juxtaposed 1,3-alternate state to form a saddle form plus a 1,3-alternate conformation. In contrast to the regular saddle form of azacalix[4]pyridine metal complexes that has

dx.doi.org/10.1021/jo301528f | J. Org. Chem. 2012, 77, 10073−10082

linear coordination vectors between pyridine ring and metal centers,[9] each coordinative pyridine ring in the **1**·$CoCl_2$ complex form an obtuse angle with the cobalt center, wherein the angle of 131° for the central bridging pyridine ring (denoted as N7) is much smaller than that of the other three ones in the range of 149−159°.

The structure of the **1**·$NiCl_2$ complex also has a metal ion inside the cavity of **1** (Figure 3b). This structure is isostructural with that of the **1**·$CoCl_2$ complex and includes a $[Ni(\mathbf{1})(CH_3OH)_2]^{2+}$ species as the cationic part and a tetrahedral $[NiCl_4]^{2-}$ ion as the anionic part. The formula of this **1**·$NiCl_2$ complex can be expressed as $\{Ni(\mathbf{1})(CH_3OH)_2\}(NiCl_4)$. The mean distance between the coordinative pyridyl nitrogen atoms and the nickel center Ni1 is 2.07 Å, a bit shorter than the mean Co−N distance of 2.10 Å in the **1**·$CoCl_2$ complex.

The structure of the **1**·$Ni(ClO_4)_2$ complex with the formula of $\{Ni(\mathbf{1})(CH_3OH)_2\}(ClO_4)_2{\cdot}CH_3OH$ is almost identical with that of the **1**·$NiCl_2$ complex but with a methanol molecule interacting with the host molecule by hydrogen bonding (O3···N11 = 2.767(3) Å) (Figure 3c).

Colorless platelike crystals of the **1**·$Cd(ClO_4)_2$ complex (the formula is $\{Cd_2(\mathbf{1})(CH_3CN)_4(H_2O)_4\}(ClO_4)_4$) were obtained by the evaporation method. It is remarkable that this **1**·$Cd(ClO_4)_2$ complex displayed a 1:2 ratio of host to metal salt. The two cadmium centers (Cd1 and Cd2 in Figure 3d) each adopts a trigonal bipyramidal geometry, wherein a pyridyl and two acetonitrile nitrogen atoms occupy the trigonal planar positions and two water molecules lie on the axial positions. The Cd−N distances are in the range of 2.208(3)−2.300(5) Å, and the summation of three N−Cd−N angles for each cadmium center is approximately 360°. Moreover, the two coordinated water molecules O2 and O3 are bridged by a perchlorate anion through hydrogen bonding (O2···O18 = 2.771 (1) Å and O3···O20 = 2.951 (1) Å). In this **1**·$Cd(ClO_4)_2$ complex, the host **1** is also in the juxtaposed 1,3-alternate conformation as similar as its unbound state. The assumption that the large ionic radius of the Cd^{2+} ion leads to the coordination difference between this cadmium complex and the Co^{2+} and Ni^{2+} complexes is partially supported by a reported complex $[(tpda)_2CdCl]NO_3$ (tpda = tripyridyldiamine), wherein the large cadmium ion is located about 1 Å above the coordination plane constituted by three pyridyl nitrogen atoms of tpda.[20]

Metal Complexation Behaviors of Host 1 in Solution. After getting two binding modes between **1** and metal ions in crystalline state, we sought to evaluate what host:guest ratio can be formed in solution between metal ions and compound **1** and to measure their association constants by UV−vis titration. The titration curves were recorded upon the gradual addition of metal perchlorate salts to the solution of **1**. All perchlorate salts were used to minimize the possible effects caused by counteranions. Titration of the host **1** by a series of tested transition metal ions including Mn^{2+}, Fe^{2+}, Co^{2+}, Ni^{2+}, Cu^{2+}, Zn^{2+}, Cd^{2+}, and Hg^{2+} all resulted in the variation of their corresponding UV−vis spectra. However, the alkali and alkaline earth metal ions such as Li^+, Na^+, K^+, Cs^+, Mg^{2+}, Ca^{2+}, and Ba^{2+} were found to have no obvious interaction with the host **1** in the UV−vis titration.

The binding interaction of **1** with $Zn(ClO_4)_2$ in solution was first investigated in view of the highly selective binding of methylazacalix[4]pyridine with Zn^{2+} in a previous report.[9] As the zinc perchlorate acetonitrile solution was gradually added to the dichloromethane solution of **1**, the main absorption bands of the free host **1** at 337 nm (the UV−vis spectra of **1**−**3** is shown in Figure S22 in the Supporting Information) decreased, and a new absorption band was generated at 323 nm (Figure 4). Four clear

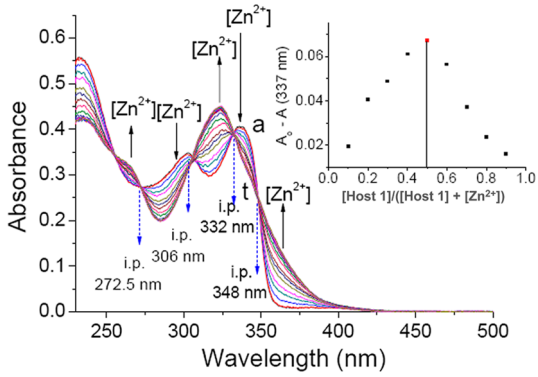

Figure 4. UV−vis titration curves of the host **1** (9.1×10^{-6} M) in a mixture of acetonitrile and dichloromethane (4:1, v/v) in response to the addition of the acetonitrile/dichloromethane (4:1, v/v) solution of $Zn(ClO_4)_2$ at 298 K. The concentrations of Zn^{2+} for curves a−t (from top to bottom) are 0, 0.9×10^{-6}, 1.8×10^{-6}, 2.7×10^{-6}, 3.6×10^{-6}, 4.6×10^{-6}, 5.5×10^{-6}, 6.4×10^{-6}, 7.30×10^{-6}, 8.2×10^{-6}, 9.1×10^{-6}, 10.0×10^{-6}, 10.9×10^{-6}, 11.9×10^{-6}, 12.8×10^{-6}, and 13.7×10^{-6} M. "i.p." is abbreviated for an isosbestic point. Inset: Job plot showing a 1:1 **1**·Zn^{2+} complex ([**1**] + $[Zn^{2+}] = 1.6 \times 10^{-5}$ M) in a mixture of acetonitrile and dichloromethane (4:1, v/v). λ_{obs} = 337 nm.

isosbestic points at 272.5, 306, 332, and 348 nm were observed in the titration curves, indicating the formation of a single new complex. The Job plot based on the absorbance at 337 nm demonstrated the formation of a 1:1 complex between **1** and zinc ion. The binding constant for the **1**−Zn^{2+} complexation was calculated to be 1.2×10^7 M^{-1} by a nonlinear least-squares fit of the titration data using a Hyperquad2003 program.[21]

We next screened a series of transition metal ions including Mn^{2+}, Fe^{2+}, Co^{2+}, Ni^{2+}, and Cu^{2+} in the third period and Cd^{2+} and Hg^{2+} in the same group with Zn^{2+} by UV−vis spectroscopic analysis (Figures S23−S29, Supporting Information). The Job plot studies revealed that the host **1** formed a 1:2 host/metal complex with Mn^{2+}, Ni^{2+}, and Hg^{2+}, although their association constants K_1 and K_2 varied within a large range. In general, the ionic radius of metal ion is an important factor that influences their binding modes with a macrocyclic polydentate ligand. In view of the crystal structure of $\{Ni(\mathbf{1})(CH_3OH)_2\}(NiCl_4)$ discussed vide supra wherein the nickel center is located inside a cavity of **1**, we expect two metal ions of Mn^{2+} or Ni^{2+} are possibly accommodated inside two cavities of the host **1**. The Hg^{2+} has the radius of 102 pm,[22] which makes itself difficult to be entrapped into the cavities of **1**. The coordination between two marginal vertical pyridine rings of **1** and metal ions maybe accounts for the 1:2 binding between **1** and Hg^{2+} according to the crystal structure of $\{Cd_2(\mathbf{1})(CH_3CN)_4(H_2O)_4\}(ClO_4)_4$). In addition, other binding modes between **1** and Hg^{2+} cannot be ruled out because not all absorption curves pass through a common point and two sets of titration curves (red and blue in Figure S29, Supporting Information) can be resolved. As shown in Table 2, among the 1:1 host/metal complexes determined by the Job plot studies the K values for Co^{2+} and Zn^{2+} are higher than the other metal ions (Fe^{2+}, Cu^{2+}, and Cd^{2+}), suggesting a better recognition effect for Co^{2+} and Zn^{2+}. The Cd^{2+} has a low K_1 value of 1.0×10^5 M^{-1}, which is comparable with the K_1 value for Hg^{2+}. This implies that the binding mode of Cd^{2+} and Hg^{2+} is possibly similar.

Consequently, three possible binding modes between the host **1** and transition metal ions can be concluded on the basis of the UV−vis titration. When the radius of the entrapped metal ions is small (such as Mn^{2+} and Ni^{2+}), a [**1**·2M] complex with metal ions

dx.doi.org/10.1021/jo301528f | J. Org. Chem. 2012, 77, 10073−10082

Table 2. Association Constants between Host 1 and Metal Ions at 298 K[a]

metal ions		1		azacalix[6]pyridine[23]
	radius[22] (pm)	K_1 (M^{-1})	K_2 (M^{-1})	K (M^{-1})
Mn^{2+}	67 (ls), 83 (hs)	$(1.23 \pm 0.03) \times 10^6$	$(8.34 \pm 0.03) \times 10^5$	–
Fe^{2+}	61 (ls), 78 (hs)	$(2.57 \pm 0.03) \times 10^6$		$(5.63 \pm 0.10) \times 10^5$
Co^{2+}	65 (ls), 74.5 (hs)	$(5.92 \pm 0.09) \times 10^7$		–
Ni^{2+}	69	$(2.68 \pm 0.03) \times 10^6$	$(1.02 \pm 0.03) \times 10^4$	$(6.32 \pm 0.06) \times 10^5$
Cu^{2+}	73	$(1.31 \pm 0.02) \times 10^6$		$(5.39 \pm 0.03) \times 10^5$
Zn^{2+}	74	$(1.25 \pm 0.08) \times 10^7$		–
Cd^{2+}	95	$(1.00 \pm 0.01) \times 10^5$		–
Hg^{2+}	102	$(5.02 \pm 0.05) \times 10^5$	$(1.53 \pm 0.05) \times 10^5$	$(4.03 \pm 0.07) \times 10^5$

[a]"ls" = low-spin state. "hs" = high-spin state. "–" = azacalix[6]pyridine has no obvious response in UV–vis spectra upon the complexation with metal ions.

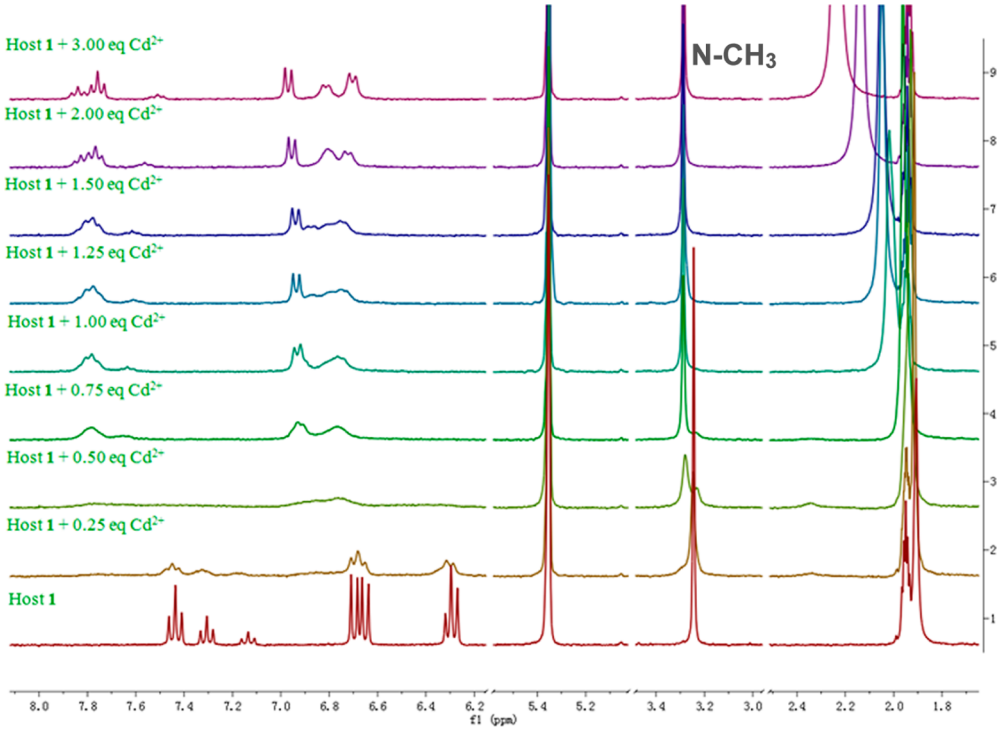

Figure 5. ^{1}H NMR spectra of the host **1** in CD_3CN/CD_2Cl_2 (v/v 2:1) in the absence and presence of different amounts of $Cd(ClO_4)_2$ at 298 K.

situated inside two cavities of **1** can be acquired. With the increasing of metal ion radius (Fe^{2+}, Co^{2+}, Cu^{2+}, and Zn^{2+}), the host **1** can only bond to a single metal ion by its one cavity as shown in the crystal structures of **1**·Co^{2+} and **1**·Ni^{2+} complexes. As to the large metal ions Cd^{2+} and Hg^{2+}, their binding mode is likely described as one or two metal ions floating on the groove of **1** generated by its four procumbent and three vertical pyridine rings. Meanwhile, in contrast to the binding constants of azacalix[6]pyridine against several metal ions (Table 2),[23] the bimacrocyclic host **1** exhibited a better metal ion affinity, indicating that the internal bridging of the large azacalixaromatic rings indeed improve their molecular recognition ability.

To elucidate the details of the binding process between **1** and metal ions, we next examined the ^{1}H NMR variation of **1** upon gradually adding metal salts of Zn^{2+}, Cd^{2+}, and Hg^{2+}. Such three metal ions are purposefully selected because they are not paramagnetic, and their ionic radii are within a wide range from 74 to 102 pm. Addition of the CD_3CN solution of $Zn(ClO_4)_2$ to the solution of **1** (2.0 mM)) in CD_2Cl_2 at 298 K led to the appearance of a new set of coupled triplet and doublet signals corresponding to the pyridyl protons at low field, indicating the occurrence of the metal:host complexation (Figure S30, Supporting Information). Proton signals corresponding to the parent bimacrocycle disappeared after an equimolar amount of $Zn(ClO_4)_2$ was added, and the singlet peak of the bridging $N-CH_3$ protons in its unbound state were split into two singlet peaks in a 1:1 ratio. Further addition of $Zn(ClO_4)_2$ did not change the NMR spectra any more, explicitly confirming the formation of the 1:1 host/metal complex in this system. In contrast, although addition of one equivalent $Cd(ClO_4)_2$ into the solution of **1** also made the proton signals of the unbound bimacrocycle disappear, the signals of the bridging $N-CH_3$ only down-shifted a little bit and preserved its singlet form (Figure 5). This means the host molecule in this **1**·$Cd(ClO_4)_2$ complex has a high symmetry. We propose that the Cd^{2+} ion is most probably hopping between two cavities of **1** at a high frequency, a process which is much faster in relative to the time scale of NMR. The metal ion hopping motion in this **1**·$Cd(ClO_4)_2$ complex was also reflected by the variable-temperature proton NMR spectra. As the probe temperature was decreased to 218 K, one singlet signal of the N-Me

dx.doi.org/10.1021/jo301528f | J. Org. Chem. 2012, 77, 10073–10082

protons was split into two singlet peaks (Figure S31, Supporting Information). Interestingly, addition of $Hg(ClO_4)_2$ to the solution of **1** in a ratio lower than 2:1 resulted in the appearance of four new singlet signals corresponding to the N−CH_3 protons (Figure S32, Supporting Information). We hypothesize this is due to the interaction of the existence of several kinds of host·metal complexes. The ESI mass spectroscopy of the mixture of Hg^{2+} and **1** in a 1:1 ratio displayed three sets of peaks for the Hg^{2+}/**1** complexation in 2:1, 1:1 and 1:2 ratio (Figure S33, Supporting Information), supporting our assumption of the coexistence of several **1**·metal species. When 2 equiv of $Hg(ClO_4)_2$ was added, the four singlets of N−CH_3 merged into only one singlet. This observation confirmed the 1:2 host/metal stoichiometry observed in the UV−vis titration.

The UV−vis titration and Job plot studies have explored that the bimacrocyclic host **1** can form 1:1 and 1:2 host/metal complexes with different transition metal ions. The crystalline solid-state structures of four acquired **1**·metal complexes demonstrated that the cavities and the marginal pyridines of **1** can be employed to trap metal ions by coordination. As shown in Scheme 3, four types

Scheme 3. Schematic Representation of Four Possible Coordination Modes of the Host 1

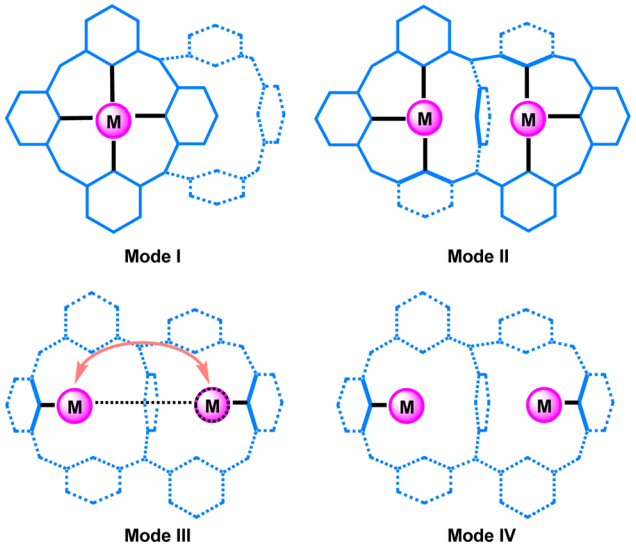

of possible coordination modes can be conceptually proposed based on the 1:1 and 1:2 host/metal stoichiometry and the two kinds of binding sites. Among them, modes I and IV have been substantiated by crystal structure studies of $\{Co(\mathbf{1})(CH_3OH)_2\}$-$(CoCl_4)\cdot 3(CH_3OH)$ and $\{Cd_2(\mathbf{1})(CH_3CN)_4(H_2O)_4\}(ClO_4)_4$), respectively. In solution, the NMR studies of the binding process between Zn^{2+}, Cd^{2+} and Hg^{2+} and **1** provide some evidence for the occurrence of mode III. The central bridging pyridine ring in **1** may facilitate the translocation of the medium-sized Cd^{2+} from one side to another side and thus accelerate the hopping frequency by use of its labile coordination, consequently resulting in mode III. Our hypothesis of the existence of mode II is mainly derived from the Job plot studies of Mn^{2+} and Ni^{2+} and crystal structures of $\{Ni(\mathbf{1})(CH_3OH)_2\}$-$(NiCl_4)$ and $\{Ni(\mathbf{1})(CH_3OH)_2\}(ClO_4)_2\cdot CH_3OH$, although solid-state structures of 1:2 host/metal complexes have not been established to date.

CONCLUSION

In summary, we have described a simple procedure for the first synthesis of 1,3-arylene-bridged azacalix[6]aromatics **1**−**3** that feature two juxtaposed 1,3-alternate macrocycles. The application of a stellated tetrabrominated pentamer in this synthesis represents an unprecedented synthetic pathway for constructing complex multicyclic heteracalixaromatic compounds. The incorporation of a 1,3-arylene bridge into the large azacalixaromatics has a profound impact on the structural and electronic properties of the resulting macrocycles, finally leading to the conformation fixation of flexible macrocycles. Binding modes between the all-pyridine host **1** and transition metal ions with different ionic radius have been established by UV−vis and NMR titration and X-ray crystallographic analysis. Four possible coordination modes between **1** and metal ions including a dynamic hopping motion potentiate the promising applications of this bimacrocyclic host in metal ion transport, ion channel, and metalloenzyme mimics and hierarchical supramolecular assembly.

EXPERIMENTAL SECTION

Methods and Materials. ^1H and ^{13}C NMR spectra were recorded on a 300 MHz spectrometer. NOESY spectra and variable-temperature NMR were recorded on a 600 MHz spectrometer. Chemical shifts are reported in ppm versus tetramethylsilane with either tetramethylsilane or the residual solvent resonance used as an internal standard. All solvents were dried or purified according to standard procedures prior to use. 2,6-Diaminopyridine **8**, benzene-1,3-diamine **9**, and 2,6-dibromopyridine **10** were commercially available. Compounds **6**, **11**, **12**, and **14** were prepared according to the literatures.[24]

7: To a solution of **11** (419 mg, 1 mmol) in dry DMF (20 mL) at room temperature was added NaH (96 mg, 4 mmol) slowly, and the mixture was stirred at room temperature. After 1 h, **10** (4.74 g, 20 mmol) and CuI (380 mg, 2 mmol) were added to the mixture slowly, and the reaction mixture was heated to 110 °C for another 12 h under argon protection and then cooled down to room temperature. Water (1 mL) was slowly added. Ethyl acetate (50 mL) was added to the mixture, and the combined solution was washed with saturated brine (3 × 50 mL). The organic phase was dried over anhydrous Na_2SO_4. After removal of solvent, the residue was chromatographed on a silica gel column (100−200) with a mixture of petroleum ether (60−90 °C) and ethyl acetate (v/v = 4:1) as a mobile phase to give pure **7** (241.9 mg, 33%) as a white solid (mp 166−167 °C): IR (KBr): ν 1551, 1571, 1417 cm^{-1}. ^1H NMR (300 MHz, $CDCl_3$): δ 7.66 (t, J = 8.0 Hz, 1H), 7.43 (t, J = 7.9 Hz, 4H), 7.16 (d, J = 7.7 Hz, 4H), 7.02 (d, J = 8.0 Hz, 4H), 6.91 (d, J = 8.0 Hz, 2H). ^{13}C NMR (75 MHz, $CDCl_3$): δ 156.1, 154.9, 140.1, 139.6, 138.7, 123.4, 117.1, 114.6. MS (ESI) m/z: 730.0 (11), 732.0 (72), 734.0 $[M + H]^+$ (100), 736.0 (68), 738.0 (15). Anal. Calcd for $C_{25}H_{15}N_7Br_4$: C, 40.96; H, 2.06; N, 13.38; Found: C, 40.71; H, 2.31, N, 13.14.

13: A mixture of **12** (8.4 g, 20 mmol), **10** (11.85 g, 50 mmol), CuI (380 mg, 2 mmol), 1,10-phenanthroline (792 mg, 4 mmol) and potassium carbonate (6.9 g, 50 mmol) in dry DMSO (100 mL) was stirred at room temperature under argon protection. After 1 h, the mixture was heated to 160 °C for another 6 h and then cooled down to room temperature. Ethyl acetate (100 mL) was added to the mixture, and the combined solution was washed with saturated brine (3 × 100 mL). The organic phase was dried over anhydrous Na_2SO_4. After removal of solvent, the residue was chromatographed on a silica gel column (100−200) with a mixture of petroleum ether (60−90 °C) and ethyl acetate (v/v = 5:1) as a mobile phase to give pure **13** (7.47 g, 51%) as a white solid (mp 187−188 °C). IR (KBr): ν 1555, 1573, 1412 cm^{-1}. ^1H NMR (300 MHz, $CDCl_3$): δ 7.44 (t, J = 7.8 Hz, 5H), 7.11−7.07 (m, 11H). ^{13}C NMR (75 MHz, $CDCl_3$): δ 156.6, 144.5, 139.7, 139.4, 131.2, 128.1, 125.9, 122.2, 114.9. MS (ESI) m/z: 729.0 (15), 731.0 (70), 733.0 $[M + H]^+$ (100), 735.0 (60), 735.0 (11). Anal. Calcd for $C_{26}H_{16}N_6Br_4$: C, 42.66; H, 2.20; N, 11.48. Found: C, 42.34; H, 2.41; N, 11.14.

1: Under argon protection, a mixture of tetrabrominated nonlinear pentamer **7** (403 mg, 0.55 mmol) and diaminated monomer **6** (137 mg, 1 mmol), $Pd_2(dba)_3$ (92 mg, 0.1 mmol), dppp (82 mg, 0.2 mmol), and sodium *tert*-butoxide (288 mg, 3 mmol) in anhydrous toluene (200 mL) was heated to reflux for 8 h. The reaction mixture was cooled to room temperature and filtered through a Celite pad. The filtrate was concentrated

Table 3. Crystallographic Data of Compounds 1−3 and Four Metal Complexes of Host 1

compd	**1**·2(CH_3OH)	**2**·0.25(CH_2Cl_2)	**3**	{Co(**1**)(CH_3OH)$_2$}($CoCl_4$)·3(CH_3OH)	{Ni(**1**)(CH_3OH)$_2$}($NiCl_4$)	{Ni(**1**)(CH_3OH)$_2$}(ClO_4)$_2$·CH_3OH	{Cd_2(**1**)(CH_3CN)$_4$(H_2O)$_4$}(ClO_4)$_4$
formula	$C_{41}H_{41}N_{13}O_2$	$C_{40.25}H_{34.5}N_{12}Cl_{0.5}$	$C_{42}H_{36}N_{10}$	$C_{44}H_{53}Cl_4Co_2N_{13}O_5$	$C_{41}H_{41}Cl_4Ni_2N_{13}O_2$	$C_{42}H_{43}Cl_2NiN_{13}O_{10}$	$C_{47}H_{53}Cl_4Cd_2N_{17}O_{20}$
FW	747.87	704.02	680.81	1103.65	1007.09	1037.50	1542.66
crystal system	monoclinic	triclinic	triclinic	triclinic	triclinic	triclinic	triclinic
space group	$P2_1/c$	*P*-1	*P*-1	*P*-1	*P*-1	*P*-1	*P*-1
a/Å	23.581(5)	10.6023(9)	10.990(2)	10.203(2)	10.231(2)	12.7471(5)	12.393(3)
b/Å	15.123(3)	13.3109(12)	12.415(2)	13.486(3)	13.510(3)	13.9306(5)	16.465(3)
c/Å	10.468(2)	13.4391(12)	13.379(3)	18.280(4)	18.245(4)	15.8655(6)	17.357(5)
α/deg	90	109.330(8)	89.992(7)	101.482(3)	102.03(3)	96.018(3)	72.312(13)
β/deg	94.086(4)	101.227(7)	81.014(5)	91.641(4)	90.96(3)	93.271(3)	82.496(16)
γ/deg	90	98.434(7)	74.842(6)	99.266(4)	99.91(3)	92.071(3)	68.093(11)
V/Å^3	3724(1)	1709.2(3)	1738.7(5)	2428.2(9)	2426.1(8)	2794.7(2)	3130(1)
Z	4	2	2	2	2	2	2
D_c/g cm^{-3}	1.334	1.409	1.300	1.509	1.379	1.375	1.637
μ/mm^{-1}	0.088	0.164	0.081	0.963	1.044	0.651	0.935
R_1[a] ($I > 2\sigma$)	0.0966	0.0602	0.0650	0.0692	0.0567	0.0677	0.0630
wR_2[b] (all data)	0.1622	0.1458	0.1526	0.1675	0.1457	0.1633	0.1567
GOF	1.188	1.007	1.068	1.096	1.067	0.988	1.071

[a] $R_1 = \sum||F_o| - |F_c||/\sum|F_o|$. [b] $wR_2 = \{\sum[w(F_o^2 - F_c^2)^2]/\sum[w(F_o^2)^2]\}^{1/2}$.

under vacuum to remove toluene, and the residue was dissolved in dichloromethane (50 mL) and washed with brine (3 × 15 mL). The aqueous phase was re-extracted with dichloromethane (3 × 15 mL), and the combined organic phase was dried over anhydrous Na_2SO_4. After removal of solvent, the residue was chromatographed on a basic alumina column (200−300) with a mixture of dichloromethane and ethyl acetate (v:v = 3:1) as a mobile phase to give the product **1** (136.6 mg, 34%) as a white solid (mp 230−231 °C). Single crystals of **1** were deposited by diffusing *n*-hexane into its dichloromethane solution. IR (KBr): ν 1568, 1423, 1284 cm^{-1}. ^{1}H NMR (300 MHz, CD_2Cl_2): δ 7.47 (t, J = 8.1 Hz, 4H), 7.38 (t, J = 7.8 Hz, 2H), 7.20 (t, J = 7.8 Hz, 1H), 6.76 (d, J = 8.1 Hz, 4H), 6.72 (d, J = 7.8 Hz, 4H), 6.39 (d, J = 7.8 Hz, 2H), 6.33 (d, J = 8.1 Hz, 4H), 3.31 (s, 12H). ^{13}C NMR (75 MHz, CD_2Cl_2): δ 158.7, 158.3, 157.5, 154.7, 139.1, 138.7, 138.0, 121.1, 120.1, 104.1, 100.6, 37.1. MS (MALDI-TOF) m/z: 684.6 [M + H]$^+$ (100), 706.7 [M + Na]$^+$ (23). Anal. Calcd for $C_{39}H_{33}N_{13}$: C, 68.51; H, 4.86; N, 26.63. Found: C, 68.56; H, 4.94; N, 26.40.

2: A similar procedure with that of compound **1** using **13** (366 mg, 0.5 mmol), **6** (411 mg, 3 mmol), $Pd_2(dba)_3$ (92 mg, 0.1 mmol), dppp (82 mg, 0.2 mmol), and sodium *tert*-butoxide (288 mg, 3 mmol) in anhydrous toluene (200 mL) produced compound **2** (173.9 mg, 51%) as a colorless crystal (mp 235−236 °C). A mobile phase of *n*-hexane, dichloromethane, and ethyl acetate (v/v/v = 5:3:1) was applied for chromatography. Single crystals of **2** were deposited by diffusing diethyl ether into its dichloromethane solution. IR (KBr): ν 1576, 1565, 1432, 1418 cm^{-1}. ^{1}H NMR (300 MHz, CD_2Cl_2): δ 7.43 (t, J = 8.1 Hz, 4H), 7.28 (t, J = 7.8 Hz, 2H), 6.81 (t, J = 8.1 Hz, 1H), 6.76 (d, J = 7.8 Hz, 4H), 6.67 (d, J = 7.8 Hz, 4H), 6.39 (dd, J = 8.1, 2.1 Hz, 2H), 6.26 (d, J = 8.1 Hz, 4H), 6.11 (t, J = 1.8 Hz, 1H), 3.28 (s, 12H). ^{13}C NMR (75 MHz, CD_2Cl_2): δ 159.1, 158.4, 155.6, 146.6, 138.7, 138.1, 129.3, 128.1, 125.7, 120.5, 103.8, 99.4, 36.8. MS (MALDI-TOF) m/z: 683.4 [M + H]$^+$ (100). Anal. Calcd for $C_{40}H_{34}N_{12}$: C, 70.36; H, 5.02; N, 24.62. Found: C, 70.16; H, 5.17; N, 24.31.

3: Compound **3** was prepared from **13** and **14** by a similar procedure to the synthesis of **2**. Quantities: **13** (366 mg, 0.5 mmol), **14** (408 mg, 3 mmol), $Pd_2(dba)_3$ (92 mg, 0.1 mmol), dppp (82 mg, 0.2 mmol), sodium *tert*-butoxide (288 mg, 3 mmol), and anhydrous toluene (200 mL). The product **3** was a colorless crystal (163.2 mg, 48%). Single crystals of **3** for X-ray analysis were obtained by the evaporation of its dichloromethane solution. Mp: 227−228 °C. IR (KBr): ν 1576, 1424 cm^{-1}. ^{1}H NMR (300 MHz, CD_2Cl_2): δ 7.43 (t, J = 8.0 Hz, 4H), 7.10 (t, J = 7.8 Hz, 2H), 6.87 (s, 2H), 6.78 (d, J = 7.8 Hz, 4H), 6.67−6.65 (m, 5H), 6.28−6.21 (m, 7H), 3.25 (s, 12H). ^{13}C NMR (75 MHz, CD_2Cl_2): δ 158.50, 158.47, 156.2, 148.1, 146.3, 138.5, 129.0, 128.4, 127.7, 124.8, 124.7, 103.3, 98.4, 39.2. MS (MALDI-TOF) m/z: 681.0 [M + H]$^+$ (100). Anal. Calcd for $C_{42}H_{36}N_{10}$·0.2CH_2Cl_2: C, 72.64; H, 5.26; N, 20.07. Found: C, 72.42; H, 5.20; N, 19.98.

*{Co(**1**)(CH_3OH)$_2$}($CoCl_4$)·3(CH_3OH).* After the dichloromethane (1.2 mL) solution of **1** (7 mg, 0.01 mmol) was mixed with the methanol solution of $CoCl_2$·6H_2O (10 mg, 0.04 mmol), *n*-hexane (1 mL) was layered above the mixture. After several days, green blocklike crystals were obtained. Yield: 53% based on **1**. IR (KBr): ν 1601, 1578, 1463, 1423 cm^{-1}. Anal. Calcd for $C_{41}H_{41}Cl_4Co_2N_{13}O_2$ (formula {Co(**1**)(CH_3OH)$_2$}($CoCl_4$)): C, 48.88; H,4.10; N, 18.07. Found: C, 48.64; H, 4.34; N, 18.31.

*{Ni(**1**)(CH_3OH)$_2$}($NiCl_4$).* Diffusion of diethyl ether into the mixed solution of **1** (7 mg, 0.01 mmol) in dichloromethane (1.2 mL) and $NiCl_2$·6H_2O (10 mg, 0.04 mmol) in methanol (1 mL) yielded green columnar crystals. Yield: 42% based on **1**. IR (KBr): ν 1603, 1582, 1450, 1426 cm^{-1}. Anal. Calcd for $C_{41}H_{41}Cl_4Ni_2N_{13}O_2$ (formula {Ni(**1**)(CH_3OH)$_2$}($NiCl_4$)): C, 48.90; H, 4.10; N, 18.08. Found: C, 48.56; H, 4.15; N, 18.28.

*{Ni(**1**)(CH_3OH)$_2$}(ClO_4)$_2$·CH_3OH.* Host **1** (7 mg, 0.01 mmol) was dissolved in dichloromethane (1 mL). Ni(ClO_4)$_2$·6H_2O (15 mg, 0.04 mmol) was dissolved in 0.5 mL methanol, which was then added into the host solution. Slow diffusion of diethyl ether into the mixture generated purplish-green prismatic crystals. Yield: 51% based on **1**. IR (KBr): ν 1601, 1584, 1451, 1426, 1087, 627 cm^{-1}. Anal. Calcd for $C_{40}H_{37}Cl_2N_{13}NiO_9$ (formula {Ni(**1**)(CH_3OH) }(ClO_4)$_2$): C, 49.36; H, 3.83; N, 18,71. Found: C,49.72; H, 3.63; N, 19.04.

*{Cd_2(**1**)(CH_3CN)$_4$(H_2O)$_4$}(ClO_4)$_4$.* Evaporation of the mixed solution of **1** (1 mg, 0.0015 mmol) in dichloromethane (1 mL) and Cd(ClO_4)$_2$·6H_2O (2.5 mg, 0.006 mmol) in acetonitrile (0.3 mL) led to colorless plate-like crystals. Yield: 32% based on **1**. IR (KBr): ν 1593, 1566, 1455, 1421, 1087, 627 cm^{-1}. Anal. Calcd for $C_{41}H_{40}Cd_2Cl_4N_{14}O_{18}$ (formula {Cd_2(**1**)(CH_3CN) (H_2O)$_2$}(ClO_4)$_4$): C, 35.59; H, 2.91; N, 14.17. Found: C,35.86; H, 2.73; N, 14.39.

X-ray Crystallography. Data for three internally 1,3-arylene-bridged azacalix[6]aromatics **1**-**3** and four coordination complexes were collected at 173 K with Mo Kα radiation (λ = 0.71073 Å) with frames of oscillation range 0.5°. All structures were solved by direct methods, and non-hydrogen atoms were located from difference Fourier maps. All non-hydrogen atoms were subjected to anisotropic refinement by full-matrix least-squares on F^2 by using the SHELXTL program. The X-Seed program[25] was used to generate the X-ray structural diagrams pictured in this paper. The parameters for the crystal data and X-ray structure analysis are summarized in Table 3. CCDC deposition numbers: **1** (900985); **2** (900986); **3** (900987); **1**·$CoCl_2$ (900988), **1**·$NiCl_2$ (900989), **1**·Ni(ClO_4)$_2$ (906857), and **1**·Cd(ClO_4)$_2$ (900991).

■ ASSOCIATED CONTENT

Supporting Information

NMR spectra data for **1**−**3**. UV and NMR titration curves for host **1** and metal ions. Crystal data of **1**−**3** and **1**·metal complexes (CIF). This material is available free of charge via the Internet at http://pubs.acs.org.

■ AUTHOR INFORMATION

Corresponding Author

*zhaolchem@mail.tsinghua.edu.cn; wangmx@mail.tsinghua.edu.cn.

Notes

The authors declare no competing financial interest.

■ ACKNOWLEDGMENTS

Financial support by the National Natural Science Foundation of China (21002057, 91127006, 21132005, 20972161, 21121004) and the National Basic Research Program of China (973 program, 2011CB932501) is gratefully acknowledged. This work is also supported by Tsinghua University Initiative Scientific Research Program.

■ REFERENCES

(1) (a) Seo, J.; Park, S.; Lee, S. S.; Fainerman-Melnikova, M.; Lindoy, L. F. *Inorg. Chem.* **2009**, *48*, 2770. (b) Cazacu, A.; Tong, C.; Lee, A. V.; Fyles, T. M.; Barboiu, M. *J. Am. Chem. Soc.* **2006**, *128*, 9541. (c) Barboiu, M.; Cerneaux, S.; van der Lee, A.; Vaughan, G. *J. Am. Chem. Soc.* **2004**, *126*, 3545. (d) Sidorov, V.; Kotch, F. W.; Kuebler, J. L.; Lam, Y. F.; Davis, J. T. *J. Am. Chem. Soc.* **2003**, *125*, 2840.

(2) (a) Kim, J. S.; Quang, D. T. *Chem. Rev.* **2007**, *107*, 3780. (b) Lindoy, L. F. *Dalton Trans.* **2006**, *43*, 5115. (c) Choi, K. H.; Hamilton, A. D. *J. Am. Chem. Soc.* **2003**, *125*, 10241. (d) Gawley, R. E.; Pinet, S.; Cardona, C. M.; Datta, P. K.; Ren, T.; Guida, W. C.; Nydick, J.; Leblanc, R. M. *J. Am. Chem. Soc.* **2002**, *124*, 13448. (e) Beer, P. D.; Gale, P. A. *Angew. Chem., Int. Ed.* **2001**, *40*, 486. (f) Yang, X. G.; Knobler, C. B.; Zheng, Z. P.; Hawthorne, M. F. *J. Am. Chem. Soc.* **1994**, *116*, 7142.

(3) (a) Oliveri, C. G.; Ulmann, P. A.; Wiester, M. J.; Mirkin, C. A. *Acc. Chem. Res.* **2008**, *41*, 1618. (b) Vigato, P. A.; Peruzzo, V.; Tamburini, S. *Coord. Chem. Rev.* **2012**, *256*, 953.

(4) Arnaud-Neu, F.; Schewing-Weill, M.-J.; Dozol, J.-F. Calixarene for Nuclear Waste Treatment. In *Calixarenes 2001*; Asfari, Z., Böhmer, V., Harrowfield, J., Vicens, J., Eds.; Kluwer Academic Publishers: Dordrecht, 2001.

(5) (a) Sliwa, W. *Chem. Heterocycl. Compd.* **2004**, *40*, 683. (b) Kumar, S.; Paul, D.; Singh, H. *Adv. Heterocycl. Chem.* **2005**, *89*, 65. (c) Wang, M.-X. *Chem. Commun.* **2008**, 4541. (d) Tsue, H.; Ishibashi, K.; Tamura, R. *Top. Heterocycl. Chem.* **2008**, *17*, 73. (e) Wang, M.-X. *Acc. Chem. Res.* **2012**, *45*, 182.

(6) (a) Sommer, N.; Staab, H. A. *Tetrahedron Lett.* **1966**, *7*, 2837. (b) Maes, W.; Dehaen, W. *Chem. Soc. Rev.* **2008**, *37*, 2393. (c) Shivanyuk, A.; Far, A. R.; Rebek, J. *Org. Lett.* **2002**, *4*, 1555. (d) Li, X.; Upton, T. G.; Gibb, C. L. D.; Gibb, B. C. *J. Am. Chem. Soc.* **2003**, *125*, 650. (e) Katz, J. L.; Feldman, M. B.; Conry, R. R. *Org. Lett.* **2005**, *7*, 91. (f) Hao, E.; Fronczek, F. R.; Vicente, M. G. H. *J. Org. Chem.* **2006**, *71*, 1233. (g) Katz, J. L.; Geller, B. J.; Foster, P. D. *Chem. Commun.* **2007**, 1026. (h) Hu, S.-Z.; Chen, C.-F. *Chem. Commun.* **2010**, 4199.

(7) (a) Ito, A.; Ono, Y.; Tanaka, K. *J. Org. Chem.* **1999**, *64*, 8236. (b) Selby, T. D.; Blackstock, S. C. *Org. Lett.* **1999**, *1*, 2053. (c) Tsue, H.; Ishibashi, K.; Takahashi, H.; Tamura, R. *Org. Lett.* **2005**, *7*, 2165. (d) Zhang, E.-X.; Wang, D.-X.; Zheng, Q.-Y.; Wang, M.-X. *Org. Lett.* **2008**, *10*, 2565.

(8) (a) Wang, M.-X.; Yang, H.-B. *J. Am. Chem. Soc.* **2004**, *126*, 15412. (b) Fukushima, W.; Kanbara, T.; Yamamoto, T. *Synlett.* **2005**, 2931.

(9) Gong, H.-Y.; Zheng, Q.-Y.; Zhang, X.-H.; Wang, D.-X.; Wang, M.-X. *Org. Lett.* **2006**, *8*, 4895.

(10) Gong, H.-Y.; Wang, D.-X.; Xiang, J.-F.; Zheng, Q.-Y.; Wang, M.-X. *Chem.—Eur. J.* **2007**, *13*, 7791.

(11) Gong, H.-Y.; Zhang, X.-H.; Wang, D.-X.; Ma, H.-W.; Zheng, Q.-Y.; Wang, M.-X. *Chem.—Eur. J.* **2006**, *12*, 9262.

(12) Anand, V. G.; Saito, S.; Shimizu, S.; Osuka, A. *Angew. Chem., Int. Ed.* **2005**, *44*, 7244.

(13) Himes, R. A.; Barnese, K.; Karlin, K. D. *Angew. Chem., Int. Ed.* **2010**, *49*, 6714.

(14) Shibasaki, M.; Kanai, M.; Matsunaga, S.; Kumagai, N. *Acc. Chem. Res.* **2009**, *42*, 1117.

(15) (a) Paul, F.; Patt, J.; Hartwig, J. F. *J. Am. Chem. Soc.* **1994**, *116*, 5969. (b) Guram, A. S.; Buchwald, S. L. *J. Am. Chem. Soc.* **1994**, *116*, 7901.

(16) (a) Berry, J. F. In *Multiple Bonds Between Metal Atoms*; Cotton, F. A., Murillo, C. A., Walton, R. A., Eds.; Springer: New York, 2005; pp 669−706. (b) Berry, J. F. *Struct. Bonding (Berlin)* **2010**, *136*, 1. (c) Yeh, C.-Y.; Wang, C.-C.; Chen, Y.-H.; Peng, S.-M. In *Redox Systems Under Nano-Space Control*; Hirao, T), Ed.; Springer: Heidelberg, 2006; pp 85−115. (d) Liu, I. P.-C.; Wang, W.-Z.; Peng, S.-M. *Chem. Commun.* **2009**, 4323−4331. (e) Ismayilov, R. H.; Wang, W.-Z.; Lee, G.-H.; Yeh, C.-Y.; Hua, S.-A.; Song, Y.; Rohmer, M.-M.; Benard, M.; Peng, S.-M. *Angew. Chem., Int. Ed.* **2011**, *50*, 2045−2048.

(17) (a) Vezzu, D. A. K.; Deaton, J. C.; Jones, J. S.; Bartolotti, L.; Harris, C. F.; Marchetti, A. P.; Kondakova, M.; Pike, R. D.; Huo, S. *Inorg. Chem.* **2010**, *49*, 5107. (b) Breivogel, A.; Foerster, C.; Heinze, K. *Inorg. Chem.* **2010**, *49*, 7052. (c) Ni, J.; Wei, K.-J.; Min, Y.; Chen, Y.; Zhan, S.; Li, D.; Liu, Y. *Dalton Trans.* **2012**, *41*, 5280. (d) Ramya, A. R.; Sharma, D.; Natarajan, S.; Reddy, M. L. P. *Inorg. Chem.* **2012**, *51*, 8818.

(18) (a) Wang, Z.-L.; Zhao, L.; Wang, M.-X. *Org. Lett.* **2011**, *13*, 6560. (b) Wang, Z.-L.; Zhao, L.; Wang, M.-X. *Org. Lett.* **2012**, *14*, 1472. (c) Wang, Z.-L.; Zhao, L.; Wang, M.-X. *Chem. Commun.* **2012**, *48*, 9418. (d) Yao, B.; Wang, Z.-L.; Zhang, H.; Wang, D.-X.; Zhao, L.; Wang, M.-X. *J. Org. Chem.* **2012**, *77*, 3336.

(19) Shieh, S.-J.; Chou, C.-C.; Lee, G.-H.; Wang, C.-C.; Peng, S.-M. *Angew. Chem., Int. Ed. Engl.* **1997**, *36*, 56.

(20) Wei, K.; Xie, Y.; Wang, X.; Zhang, M.; Liu, Q.; Peng, S. *Appl. Organomet. Chem.* **2005**, *19*, 178.

(21) Gans, P.; Sabatini, A.; Vacca, A. *Talanta* **1996**, *43*, 1739.

(22) Shannon, R. D. *Acta Crystallogr.* **1976**, *A32*, 751.

(23) Zhang, E.-X. Ph.D. Dissertation, Institute of Chemistry, Chinese Academy of Sciences, Beijing, 2009 (in Chinese).

(24) Yao, B.; Wang, D.-X.; Gong, H.-Y.; Huang, Z.-T.; Wang, M.-X. *J. Org. Chem.* **2009**, *74*, 5361.

(25) (a) Barbour, L. J. *J. Supramol. Chem.* **2001**, *1*, 189. (b) Atwood, J. L.; Barbour, L. J. *Cryst. Growth Des.* **2003**, *3*, 3.